Structure Functions at HERA - Status and Future

Max Klein[a]

[a] DESY, Platanenallee 6, 15738 Zeuthen, Germany, E-mail: klein@ifh.de

A brief overview is given on results and prospects of nucleon structure function measurements at HERA.

1. Introduction

Structure functions characterize the partonic structure of the proton. In Quantum Chromodynamics (QCD) structure functions are defined as convolutions of coefficient functions for the exchanged boson-parton interaction with parton momentum distributions $q(x, Q^2)$ inside the proton, where x is the fraction of proton momentum carried by the parton of type q. At large momentum transfers Q^2 and not too small x, QCD allows the perturbative calculation of the coefficient functions and predicts a logarithmic dependence (evolution) of the proton structure functions with Q^2 to higher orders in the strong coupling constant α_s. Thus precision measurements of structure functions allow perturbative QCD to be precisely tested. This is necessary to search for new physics beyond the standard partonic interactions and to find the application limits of perturbative QCD, for example at low x where the parton density was found by the HERA experiments H1 and ZEUS to be surprisingly high. The low x behaviour of the structure functions has to be known to understand high energetic cosmic neutrino interactions.

Partons are quarks and gluons which enter different structure functions and their Q^2 derivatives differently. Thus the exploration of nucleon structure requires a variety of structure functions to be accurately measured in a wide kinematic range. This requirement is ideally met by the high energy DIS collider experiments which so far have been analysing electron and positron-proton scattering data of about $20\,\mathrm{pb}^{-1}$ and $120\,\mathrm{pb}^{-1}$ luminosity, respectively, taken in the first phase of HERA.

The coupling constants of the electromagnetic, weak and strong interactions are expected to reach a unification point at very high energies which is of great interest for unified field theories as those based on supersymmetry. $\alpha_s(M_Z^2)$ is by far the least accurately measured coupling constant although deep inelastic lepton-nucleon scattering (DIS) experiments are best suited to measure it precisely [1].

This report describes structure function results obtained so far at HERA and demonstrates the big unexplored potential of its future high luminosity operation by varying the main parameters: i) the lepton-beam polarisation to measure e.g. the helicity dependence of the charged current cross section testing the chirality of the standard model or the ratio of down-to-up quark distributions, d/u, at large x, ii) the proton beam energy to measure the longitudinal structure function $F_L(x, Q^2)$ and iii) the nucleon beam particle, using eD (and later eA) instead of ep collisions, which is a necessity in exploring the partonic structure of the nucleon sea, and of the valence quark region.

Important further [2] proton structure function results are obtained in semi-inclusive analyses of deep-inelastic charm production, in diffractive and polarised DIS and in Compton scattering leading to parton distribution correlation functions. Impressive theoretical and experimental developments show that pQCD is applicable to a wider class of structure functions, and to the final state, giving important further insight in the structure of the proton and the secrets of QCD. We are yet far from understanding the richness of strong interactions, the confinement of partons and the physics of high parton density states.

2. Low Q^2, x - F_2 and F_L

At low momentum transfers Q^2 the inclusive measurements determine a cross section which in Born approximation and reduced form is given as

$$\frac{Q^4 x}{2\pi\alpha^2 Y_+} \cdot \frac{d^2\sigma}{dx dQ^2} = \sigma_r = F_2 - \frac{y^2}{Y_+} \cdot F_L. \qquad (1)$$

Here y is the inelasticity which is related to x and Q^2 as $y = Q^2/sx$. The beam energies determine the energy squared s in the centre of mass system, $s = 4E_e E_p$, and Y_+ is defined as $1 + (1-y)^2$. In the region of inelasticity below $y \simeq 0.6$ the contribution of the longitudinal structure function $F_L(x, Q^2)$ is small because positivity of cross sections requires $F_L \leq F_2$. It has thus been convention by H1 to limit data on the proton structure function $F_2(x, Q^2)$ to $y \leq 0.6$.

A selection of HERA measurements of σ_r at low x from ZEUS and H1 is shown in Fig. 1. The most recent, preliminary H1 data [3] taken with shifted vertex position in 2000 agree well with the 1999 nominal vertex data in the region of overlap, extending the measurement to lower Q^2. In this region they approach the ZEUS BPT data using the Backward Pipe Detector [5] placed downstream the positron beam direction. Lowest Q^2 data on F_2 from both collaborations are still being analyzed which will cross check the other collaboration's results. For Q^2 beyond 5 GeV^2 both H1 and ZEUS have published consistent F_2 measurements [6,7].

In the low Q^2 region, from about 0.3 to 30 GeV^2, the cross section at low x is now measured at HERA to about 3% accuracy, apart from the edges of the y range, because of physics background at high $y \geq 0.5$ and final state particle losses and electron energy resolution deterioration at low $y \leq 0.01$.

The H1 cross section data cover a y region up to 0.9 which is a most remarkable result as it requires electron identification in a hadronic background environment down to energies of 3 GeV using high resolution calorimetry and tracking. At large y effects of the longitudinal structure function are observed leading to a taming of the cross section rise towards low x and eventually its turn over for x corresponding to about $y = 0.7$, see Fig. 1. Based on the measurement of the x dependence of $F_2(x, Q^2)$, H1 has determined F_L at smallest x using different extrapolation techniques of $F_2(x, Q^2)$ into the high y kinematic region. The results obtained so far are illustrated in Fig. 2. The measured longitudinal structure function is found to be large, as expected from pQCD fits to F_2 since $F_L \propto \alpha_s \cdot xg$. Good agreement is found but a higher accuracy for $F_L(x, Q^2)$ and data at lower Q^2 and in a wider range of x are needed.

3. The High Density Parton Regime

The large values observed for $F_2(x, Q^2)$ at low x imply a high quark density since to leading order $F_2 = x \sum q + \overline{q}$. Moreover, the rapid rise of the structure function $F_2(x, Q^2)$ with Q^2 at fixed, low x and the large values determined for $F_L(x, Q^2)$ suggest that the gluon momentum density $xg(x, Q^2)$ in the proton is large at low x. Unfortunately xg cannot be observed but is derived and defined within specific choices of how to parameterise and formulate pQCD, regarding the heavy flavour treatment in particular [8]. Moreover, considerable arbitrariness is observed in global and experimental fit analyses of the x behaviour of xg at low $Q^2 \simeq 1$ GeV^2. In this region the sharing of proton momentum between sea quarks and protons is suddenly exchanged: while for Q^2 below 1 GeV^2 the gluon distribution approximately vanishes at low x, it dominates completely the scaling violations at larger Q^2 values even close to this "phase transition". Perturbative QCD fits are thus usually restricted to $Q^2 > 1$ GeV^2 and fail below, see Fig. 1 and [9]. Even restricting the analyses to the truely DIS region, i.e. larger Q^2 where $\alpha_s < 1$, leads to a change of the resulting xg as is illustrated in Fig. 3. It is thus to be emphasized that the transition from the long distance to short distance regime is not understood yet and not measured precisely enough.

From the observed independence of the local derivatives $(\partial F_2/\partial \ln x)_{Q^2}$ it has been deduced by H1 [10] that F_2 can be approximately represented as a simple form $F_2(x, Q^2) = c(Q^2) \cdot x^{-\lambda(Q^2)}$. The result of the determinations of the coefficent $c(Q^2)$ and of the function $\lambda(Q^2)$ is shown in Fig. 4. Approximately $c = const$ and $\lambda = a\ln[Q^2/\Lambda^2]$ for $Q^2 \geq 3$ GeV^2. It is amusing to see that $\Lambda \simeq \Lambda_{QCD}$ and that the function $\lambda(Q^2)$ is equal to 0.08, the soft physics limit, for $Q^2 = 0.35$ GeV^2, at the initial scale of the GRV ansatz [11]. Further constraints are required, in particular data on F_L, and higher precision in order to understand this transition which leads HERA physics to another strong interaction regime of high parton densities [12] at large or even small coupling constant.

4. DIS and the Measurement of α_s

HERA has a unique possibility to measure α_s in inclusive DIS because of the wide kinematic range covered by the collider experiments. The only missing region is medium Q^2, large x which is covered most precisely by the muon-nucleon scattering data of the BCDMS collaboration. The pQCD evolution equations relate the evolution of $F_2(x, Q^2)$ and of $\alpha_s(Q^2)$ to the quark and gluon densities. While in jet physics, for example, α_s can only be determined assuming xg to be known, in inclusive DIS one can simultaneously obtain a measurement of α_s, $xg(x, Q_0^2)$ and their correlation to each other and to the behaviour of the quark momentum distributions. Both H1 and ZEUS have recently published measurements of $\alpha_s(M_Z^2)$. The assumptions and procedure are rather maximally different.

H1 has introduced a novel flavour decomposition of F_2 which avoids deuteron data and minimizes the number of parton distributions to be fitted to two. The data are from H1 and BCDMS only which yield consistent results on $\alpha_s(M_Z^2)$, see Fig. 5, and thus allow for a mathematically firm error treatment. The result in NLO QCD is one of the most precise measurements of $\alpha_s(M_Z^2) = 0.1150 \pm 0.0017(exp) \pm 0.0008(mod)$. It yields a low xg at large x in contradiction to high E_T jet data from the Tevatron but in a consistent way regarding comparative analyses and the untolerable increase in χ^2 when xg is forced to be large at large x.

ZEUS uses the conventional quark distributions (u_v, d_v and sea) and imports the x dependence of $\bar{d} - \bar{u}$ from a global fit. The analysis is extended to lepton-proton and deuteron data from BCDMS, NMC and E665 and also to xF_3 data from the CCFR neutrino scattering experiment. The systematic errors in this multi data set analysis, and some valence quark parameters are fixed in the fit. The NLO QCD result is $\alpha_s = 0.1166 \pm 0.0008(unc) \pm 0.0032(cor) \pm 0.0036(norm) \pm 0.0018(mod)$. This and the gluon distribution are consistent with the H1 result.

Both analyses observed a too large variation of χ^2 when the renormalisation scale is varied between $Q^2/4$ and $4Q^2$. From here H1 derives an α_s uncertainty of ± 0.005 which dominates the error. ZEUS allows only half of the scale variation which gives an uncertainty of ± 0.004 the numerical difference to H1 being likely connected with the inclusion of low Q^2, large x data. Yet, the present convention allows an estimate of the sensitivity to higher-order effects rather than representing a genuine error since the amount of scale variation considered is arbitrary. Next big steps are an attempt to further improve the measurement accuracy and the completion [13] and inclusion of next-to-NLO calculations. Since the BCDMS data are of crucial importance it is considered necessary to measure the medium Q^2, larger x region at HERA which requires to lower the proton beam energy.

5. High Q^2, Neutral and Charged Currents

The large accelerator energy of HERA, $s = Q^2_{max} \simeq 10^5$ GeV^2, allows parton distributions to be measured up to very large Q^2, beyond the propagator masses squared of the W and Z. When HERA was proposed, nearly 20 years ago, it was not known whether the neutral (NC) and charged current (CC) interactions, and the electromagnetic and weak NC, would be of comparable strength at high $Q^2 \sim M^2_{Z,W}$. This has been demonstrated with the HERA data at increasing accuracy. In Fig. 6 all cross sections are seen to reach similar size while, for example, still at $Q^2 = 100$ GeV^2 the photon-exchange cross section is nearly three orders of magnitude larger than the W-exchange cross section.

Both ZEUS [9] and H1 [14] have recently presented new measurements of structure functions at large Q^2. These measurements are of interest to study the evolution in Q^2 over an unprecedented range. Both collaborations are commencing a programme of mapping the partonic nucleon structure in the newly accessed range, up to largest Q^2, corresponding to distances as small as 10^{-18} m, and down to very small x.

Examples for recent high Q^2 structure function measurements are: new data of F_2 at large x extending by far the BCDMS measurements (Fig. 7), first results [15,16] on the $\gamma - Z$ interference structure function xF_3 (Fig. 8) and new results on the CC cross section (Fig. 9). These data allow parton distribution determinations, which presently, however, still require input from other experiments and assumptions on certain parameters, like $(\bar{d} - \bar{u}) \rightarrow 0$ at low x. These assumptions have a large, often hidden influence on the parton distribution uncertainties. This field is rapidly developing. From HERA it requires high luminosity, lower energy runs and deuterons, exploiting the potential of the machine and to understand proton structure at the necessary detail and precision. This includes investigating the heavy flavour structure of the proton [8] and the untested hypothesis of intrinsic charm [19].

6. Future Measurements

The luminosity increase and use of lepton polarisation will allow to measure the electroweak structure functions [20] much more precisely than so far at HERA. In NC this concerns besides F_2 the lepton beam charge asymmetry which essentially determines the $\gamma - Z$ interference part xG_3 of the generalised structure function $\mathbf{xF_3}$. Variation of the lepton beam helicity determines the so far unmeasured structure function, $G_2 = 2x \sum e_q v_q (q + \overline{q})$, which is the $\gamma - Z$ interference part of the generalised structure function $\mathbf{F_2}$. Both $xG_3 \propto 2u_v + d_v$ and G_2 which at high x is proportional to $u_v + d_v$ will provide important information on the valence-quark distributions independently of nucleon corrections. Since the underlying asymmetries rise with Q^2 and the valence quarks drop like a power of $(1-x)$, the luminosity requirement to access high x exceeds significantly the current goal of $1\,\mathrm{fb}^{-1}$of the HERA luminosity upgrade. A similar conclusion can be drawn from a simulation of the future CC inclusive cross section measurements, see Fig. 10.

Perturbative QCD evolution and gluon splitting cannot explain a breaking of isospin symmetry in the antiquark distributions. However, in the DIS region, for $x \sim 0.05$, the difference $\bar{d} - \bar{u}$ was measured to be different from zero. The nonperturbative structure of the nucleon is seemingly more complex than a three-quark bound state. Yet, parton distribution fits assume that symmetry is restored at lower x. This, however, has not been tested but is central to the understanding of the high density parton regime and also of the true pdf uncertainty bands obtained in those fits. The rise of $F_2(x, Q^2)$ towards low x at HERA has been observed but not really understood: neither has the basic QCD dynamics been established nor are the parton distributions xg, $\bar{u}$ and $\bar{d}$ uniquely determined at low x and Q^2. While the gluon distribution needs accurate data on F_L in this region, disentangling the sea quarks and measuring the x dependence of $\bar{u}$ and $\bar{d}$ requires electron-deuteron data from HERA.

A sequence of runs at lowered E_p energies, with luminosities $\mathrm{O}(10)\mathrm{pb}^{-1}$ will allow the x dependence of $F_L(x, Q^2)$ to be measured. The energy dependence of the photoproduction background and precision tracking in front of high resolution calorimetry should permit this dominating source of uncertainty to be controlled a few times more accurately than hitherto leading to a possible measurement of $F_L(x, Q^2)$ to 5-10% accuracy, see Fig. 11.

Deuterons provide complementary information to ep scattering. This allows the $c - s$ quark distribution to be determined directly from the difference of $3 \cdot F_2$ and the CC structure function $W_2 \cdot 5/6$, based on about $50\,\mathrm{pb}^{-1}$luminosity in eD scattering [21]. With less luminosity one can measure the $\bar{d} - \bar{u}$ asymmetry at low x to a few per cent accuracy as is illustrated in Fig. 12.

REFERENCES

1. W. van Neerven, in " THERA: Electron-Proton Scattering at $\sqrt{s} \sim$ 1TeV", DESY-

01-123F vol.4, LC-REV-2001-062, p.256.
2. A. Eskreys, J. Kwiecinski and J. Szwed, eds., Proceedings, 10th International Workshop, Dis 2002, Krakow, Poland, April 2002, Acta Phys. Pol. **B 33** (2002) 2727.
3. H1 Collaboration, C. Adloff et al., Contribution 79 to EPS, Budapest, August 2001 and Contribution 975 to ICHEP, Amsterdam, August 2002, to be published.
4. T. Laštovička, Eur. Phys. J. **C 24**, (2002) 529 [hep-ph/0203260].
5. ZEUS Collaboration, J. Breitweg et al., Phys. Lett. **B 487** (2000) 53 [hep-ex/0005018].
6. C. Adloff et al., Eur. Phys. J. **21** (2001) 33 [hep-ex/0012053].
7. ZEUS Collaboration, S. Chekanov et al., Eur. Phys. J. **21** (2001) 443 [hep-ex/0105090].
8. J. Amundson et al., JHEP **0010** (2000) 031 [hep-ph/0005221] and refs therein.
9. ZEUS Collaboration, S. Chekanov et al., hep-ex/0208023, to be published.
10. H1 Collaboration, C. Adloff et al., Phys. Lett. **B 520** (2001) 183 [hep-ex/0108035].
11. M. Glück, E. Reya and A. Vogt, Z. Phys. **C 67** (1995) 433.
12. E. Iancu, A. Leonidov and L. D. McLerran, Nucl. Phys. A **692** (2001) 583 [hep-ph/0011241].
13. J. A. Vermaseren, S. Moch and A. Vogt, hep-ph/0211296, these proceedings.
14. H1 Collaboration, C. Adloff et al., Contribution 978 to ICHEP, Amsterdam, August 2002, to be published.
15. H1 Collaboration, C. Adloff et al., Eur. Phys. J. **19** (2001) 269 [hep-ex/0012052].
16. ZEUS Collaboration, S. Chekanov et al., hep-ex/0208040, to be published.
17. ZEUS Collaboration, S. Chekanov et al., Phys. Lett. **B 539** (2002) 197 [hep-ex/0205091].
18. V.N. Gribov, Zh. Exp. Teor. Fiz. **57** (1969) 1309; Sov. Phys. JETP **30** (1970) 709;
M. Strikhman, private communication.
19. S. Brodsky et al., Phys. Lett. **B93** (1980) 451.
20. M. Klein and T. Riemann, Z. Phys. **C 24** (1984) 151.
21. J. Blümlein et al., Physics at HERA, Proc. Workshop 1987, p79.

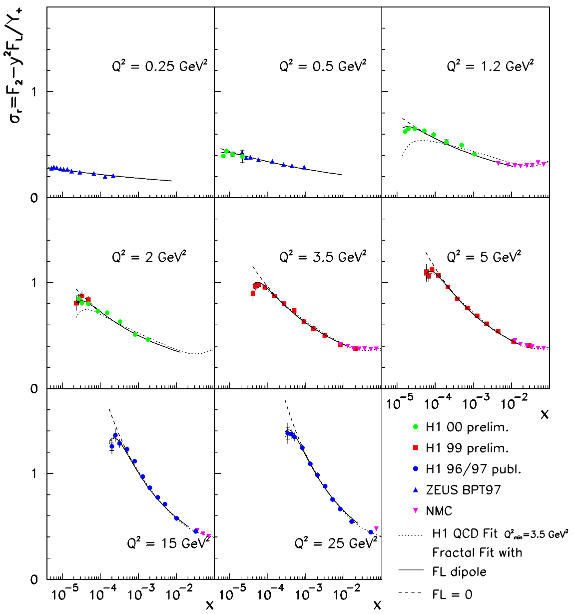

Figure 1. HERA measurements of the inclusive DIS cross section - in order increasing with Q^2: data from ZEUS (BPT97 blue triangles), H100 shifted vertex data (green points), and H199 nominal vertex data (red squares), H197 data (blue points) and, for some bins, from NMC (purple triangles). The curves are a phenomenological parameterisation of the cross section calculating F_2 within the fractal proton structure concept [4] and using a dipole model prediction for F_L (solid) and $F_L = 0$ (dashed). The dotted curves represent the NLO pQCD fit to the H197 data. The extrapolation to lower Q^2, from $Q^2_{min} = 3.5$ GeV^2 fails to describe data at about 1 GeV^2.

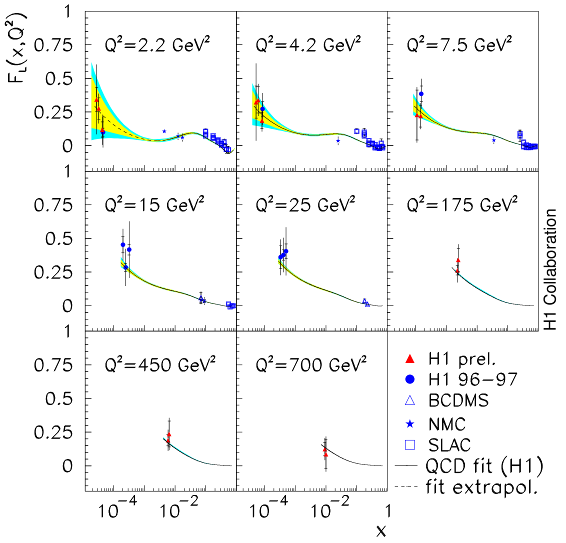

Figure 2. Measurements of $F_L(x,Q^2)$ by the H1 collaboration.

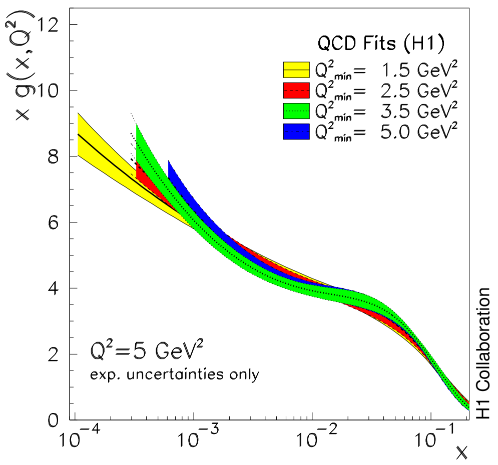

Figure 3. Effect of the Q^2_{min} cut, applied in the DGLAP QCD fit to the H1 data, on the gluon distribution at $Q^2 = 5$ GeV^2. The distributions are shown down to x values corresponding to twice the minimum x values of the data which allow a Q^2 slope to be measured.

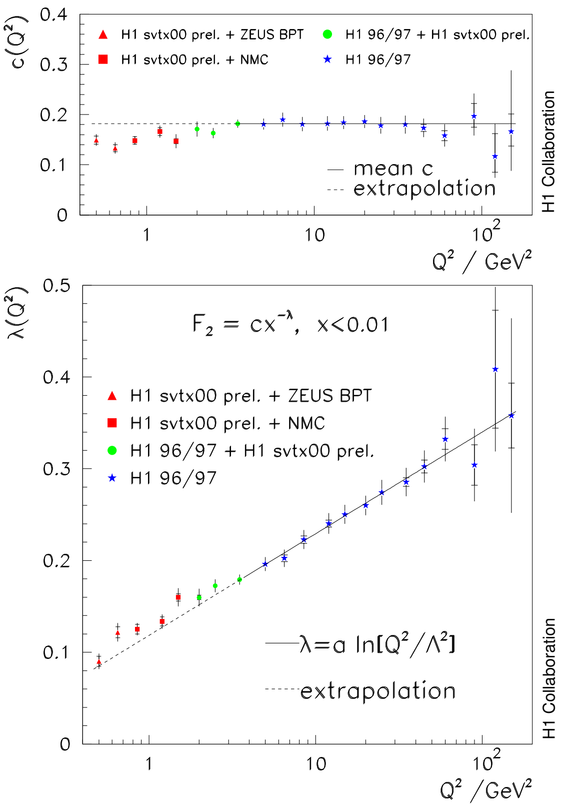

Figure 4. Determination of the coefficients $c(Q^2)$ (upper plot) and of the exponents $\lambda(Q^2)$ (lower plot) from fits of the form $F_2(x,Q^2) = c(Q^2)x^{-\lambda(Q^2)}$ for $x \leq 0.01$ using H1 data partially combined with ZEUS BPT data [5] at low Q^2 and with NMC data. The inner error bars illustrate the statistical uncertainties, the full error bars represent the statistical and systematic uncertainties added in quadrature. The straight lines represent the mean coefficient c (upper plot) and a fit of the form $a\ln[Q^2/\Lambda^2]$ (lower plot), respectively, using data for $Q^2 \geq 3.5$ GeV^2.

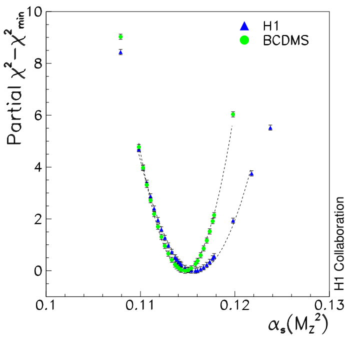

Figure 5. Partial χ^2 contributions of the H1 and BCDMS proton data in the fit to determine α_s using data from both experiments.

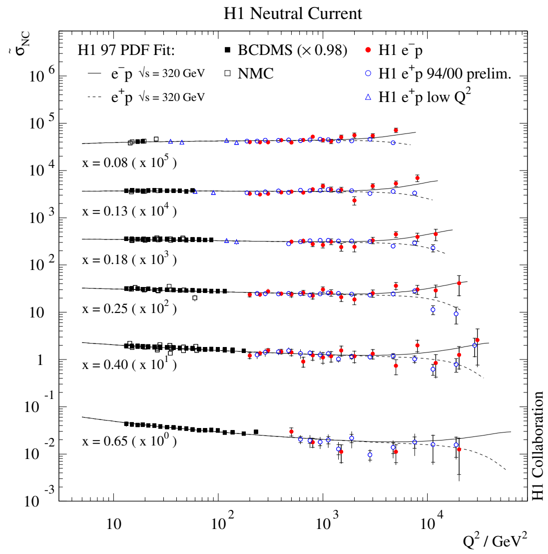

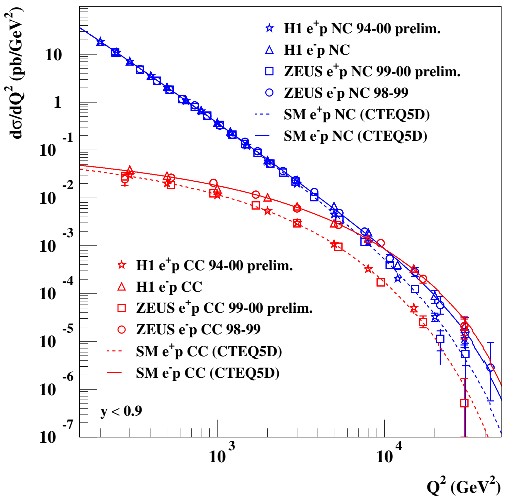

Figure 6. Measurements by H1 and ZEUS of the NC and CC cross sections in inclusive $e^{\pm}p$ scattering as functions of Q^2. At $Q^2 \simeq M_Z^2$ the NC and CC cross sections are observed to be of similar strength as had been predicted from γ, Z and W exchange calculations in the standard electroweak theory.

Figure 7. Measurements of the inclusive NC cross section at high Q^2 by H1 using e^-p (closed circles) and e^+p data (open circles), representing the total set of high Q^2 data taken in the first phase of HERA. The data are compared with the data at lower Q^2 from H1 (triangles) and fixed target μp scattering data (squares). The measurements are well described by pQCD fits.

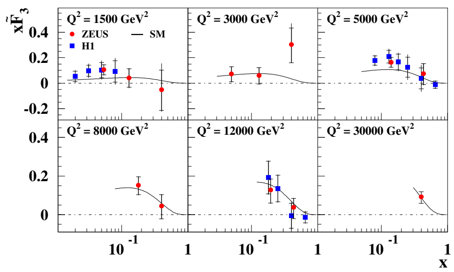

Figure 8. Measurements of the structure function xF_3 in neutral current $e^{\pm}p$ scattering at HERA, by the ZEUS and the H1 Collaborations, compared with a ZEUS NLO QCD parton-distribution fit [16].

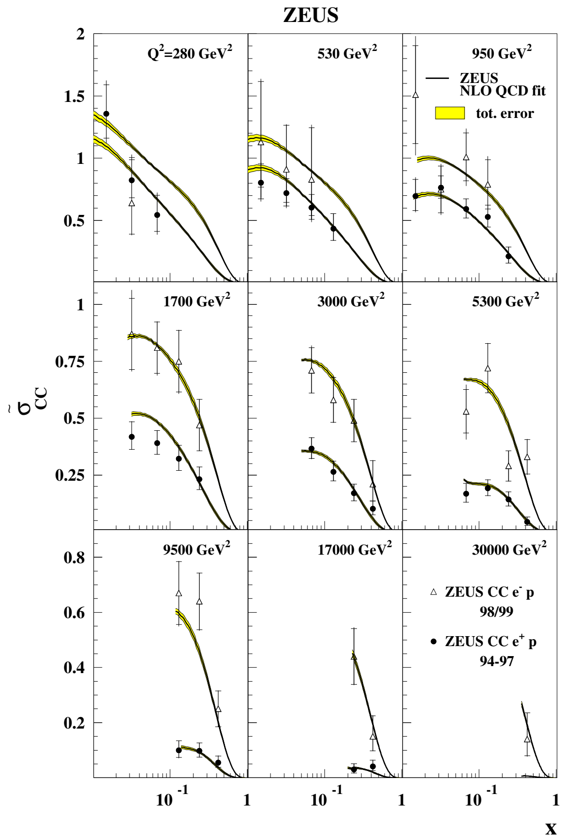

Figure 9. Measurements of the inclusive charged-current cross section at high Q^2 by the ZEUS Collaboration using electron-proton (open triangles) data at $\sqrt{s} = 318\,\mathrm{GeV}$ and positron-proton data (closed circles) at $\sqrt{s} = 300\,\mathrm{GeV}$. The curves represent a NLO QCD fit by ZEUS to neutrino and neutral-current charged lepton-nucleon scattering data. The bands are the total experimental uncertainty, from uncorrelated and correlated sources.

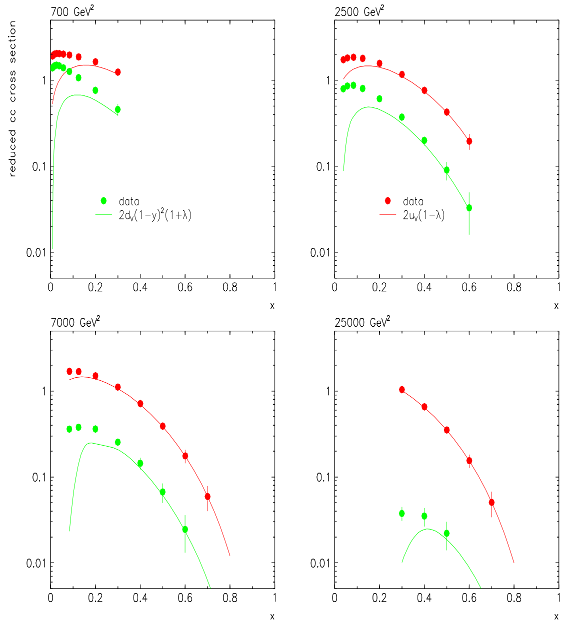

Figure 10. Simulation of future $e^{\pm}p$ charged current cross section measurements for polarisation $\lambda = \pm 1/2$ for $250\,\mathrm{pb}^{-1}$per charge state. The e^+p (reduced) CC cross section tends to $(1-y)^2 d_v$ while the larger e^-p (reduced) CC cross section approaches u_v. The HERA ep CC data determine the ratio d/u at large x free of nuclear corrections. Yet a much larger luminosity than $1\,\mathrm{fb}^{-1}$is needed to reach the high x region beyond 0.7.

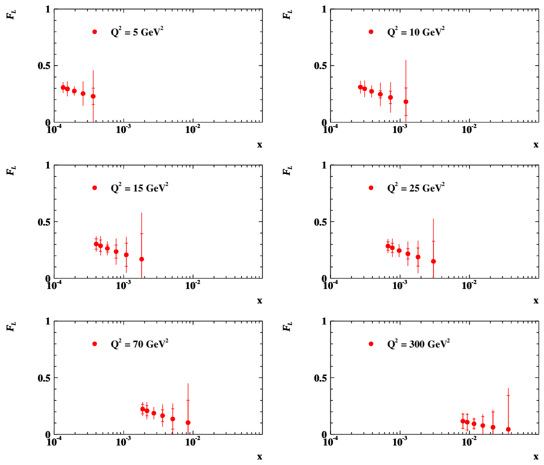

Figure 11. Simulation of a measurement of the longitudinal structure function $F_L(x, Q^2)$ with the H1 detector in its current (2002) configuration which excludes the region near $Q^2 \sim 1$ GeV^2. The x dependence is measured by variing the proton beam energy in steps of equidistant $f(y) = y^2/Y_+$ with $Y_+ = 1 + (1-y)^2$, e.g. 400, 465, 575 and 920 GeV, with a luminosity of $10\,\mathrm{pb}^{-1}$ at each energy. The inner errors are the statistical uncertainty, the total error the full uncertainty taking into account the systematic error correlations in the extraction of F_L. The accuracy is best for a maximum range of E_p and largest possible y, taken to be 0.9 as achieved by H1 using the backward silicon tracker.

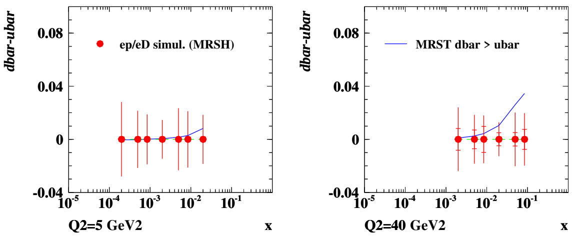

Figure 12. Simulation of the difference $\overline{d}$ - $\overline{u}$ using $40\,\mathrm{pb}^{-1}$ of ep and $20\,\mathrm{pb}^{-1}$ of eD data to determine $F_2(p)$ and $F_2(N)$ which allows to test the sea symmetry at low x. The inner error bars are the statistical error and the outer error bars include the systematic errors as currently achieved in low x F_2 measurements by H1. The difference at low x is unknown. The simulated data points are positioned at MRSH (zero difference). Measurements of the Gottfried sum rule and Drell Yan data determined $\overline{d}$ - $\overline{u}$ to be positive at medium x which changed pdf fits (e.g. MRST PDFLIB code 3,75, blue,solid line). An uncertainty of this measurement arises from shadowing which is linked to diffraction and thus controllable rather accurately [18].